

## Solubility and Dissolution Enhancement of Atorvastatin Calcium using Phospholipid Solid Dispersion Technique #

Bashar K. K. Ghyadh<sup>\*,1</sup> and Eman B. H. Al-Khedairy<sup>1</sup>

#2nd Scientific Conference for Postgraduate Students Researches.

\*Department of Pharmaceutics, College of Pharmacy, University of Baghdad, Baghdad, Iraq.

### Abstract

Atorvastatin (ATR) is a poorly water-soluble anti-hyperlipidemic drug. The drug belongs to the class II group, according to the biopharmaceutical classification system (BCS), with low bioavailability due to its low solubility. Solid dispersion is an effective technique for enhancing the solubility and dissolution of drugs. Phosphatidylcholine (PC) was selected as an unusual carrier for ATR due to its lipid-lowering effect to prepare phospholipid solid dispersion (PSD) with or without adsorbent (magnesium aluminium silicate, silicon dioxide 15nm, silicon dioxide 30nm, calcium silicate) was used to prepare ATR PSD using different drug: PC: adsorbent ratios by solvent evaporation method. The resulted PSD was evaluated for its percentage yield, drug content, solubility, dissolution rate, Fourier transformation infrared spectroscopy (FTIR), powder X-ray diffraction study (PXRD), and differential scanning calorimetry (DSC). The prepared (PSD) showed improvement in drug solubility in all prepared formulas. The best result was obtained with F5 (ATR: PC: MAS 1:3:4). The solubility was increased by 21 folds compared to the pure drug with enhanced dissolution and decreased crystallinity, as confirmed by DSC and PXRD. While FTIR results indicate compatibility between the drug and the excipients.

**Keywords:** Atorvastatin, Phospholipid Solid dispersion, Phosphatidylcholine, Magnesium aluminium silicate.

### تحسين الذوبانية ومعدل الذوبان للأتورفاستاتين كالمسيوم باستخدام تقنية المنتشر الصلب باستخدام الشحم الفسفوري #

بشار كريم كاظم<sup>\*</sup>،<sup>1</sup> و ايمان بكر حازم الخضير<sup>1</sup>

#المؤتمر العلمي الثاني لطلبة الدراسات العليا  
\*فرع الصيدلانيات، كلية الصيدلة، جامعة بغداد، بغداد، العراق.

### الخلاصة

الأتورفاستاتين هو دواء مضاد للدهون الزائدة في الدم ذو قابلية ضعيفة للذوبان في الماء. ينتمي الدواء إلى المجموعة الثانية وفقاً لنظام التصنيف الحيوي الصيدلاني بسبب بسبب قلة ذوبانه. يعد المنتشر الصلب تقنية فعالة لتحسين قابلية الذوبان وسرعة الذوبان للأدوية. تم اختيار فوسفاتيديل كولين كامل للأتورفاستاتين نظراً لتأثيره الخافض للدهون لتحضير المنتشر الصلب مع أو بدون ممتز (سيليكات المنيوم المغنيسيوم، ثاني أكسيد السيليكون 15 نانومترًا، ثاني أكسيد السيليكون 30 نانومترًا، سيليكات الكالسيوم) لإعداد المنتشر الصلب الشحمي باستخدام نسب مختلفة من الدواء: الفوسفاتيديل كولين: ممتز بطريقة تبخير المذيب. تم تقييم المنتشر الصلب الشحمي الناتج من حيث النسبة المئوية المستحلبة، ومحتوى الدواء، وقابلية الذوبان، وسرعة الذوبان، مطياف الأشعة تحت الحمراء، والهيكل البلوري باستخدام تقنية حيود الأشعة السينية ومسر المسح التبايني. أظهر المنتشر الصلب الشحمي المحضر تحسناً في قابلية ذوبان الدواء في جميع التركيبات المحضرة. تم الحصول على أفضل نتيجة مع F5 (أتورفاستاتين: فوسفاتيديل كولين: سيليكات المنيوم المغنيسيوم) بنسبه 1:3:4 حيث زادت قابلية الذوبان بمقدار 21 ضعفاً مقارنة بالدواء النقي مع تحسين سرعة الذوبان وانخفاض الحالة البلورية كما أكد مسعر المسح التبايني و حيود الأشعة السينية. بينما تشير نتائج مطياف الأشعة تحت الحمراء إلى التوافق بين الدواء والمضافات.

الكلمات المفتاحية: الأتورفاستاتين، المنتشر الصلب الشحمي، فوسفاتيديل كولين، سيليكات المنيوم المغنيسيوم.

### Introduction

Poor aqueous solubility is one of the most frequently encountered problems for drug substance formulation. The low solubility leads to a very slow drug dissolution rate and poor intestinal absorption<sup>(1)</sup>. The bioavailability of BCS class II drugs is likely to be dissolution rate limited. The BCS class II drugs have been on focus for solubility enhancement researches, and several formulation approaches for this class of compounds have been developed<sup>(2)</sup>.

Atorvastatin is a 3-hydroxy-3-methylglutaryl coenzyme A (HMG-CoA) reductase inhibitor; it is a lipid-regulating drug with actions on plasma lipids similar to those of simvastatin. It is

also used for primary and secondary prophylaxis of cardiovascular events<sup>(3)</sup>. Atorvastatin (Figure 1) is a white or almost white powder. Very slightly soluble in water, slightly soluble in alcohol, practically insoluble in dichloromethane. It has log P 6.36 and an absolute oral bioavailability of 12%. The poor oral bioavailability is attributed to presystemic clearance in the gastrointestinal mucosa, high hepatic first-pass metabolism, and low water solubility<sup>(4,5)</sup>. Many techniques were utilized to enhance the aqueous solubility of ATR including nanosuspension and complexation with cyclodextrin<sup>(6,7)</sup>.

<sup>1</sup>Corresponding author E-mail: bashaar.kareem2100m@copharm.uobaghdad.edu.iq

Received: 31/5/2023

Accepted: 31/7/2023

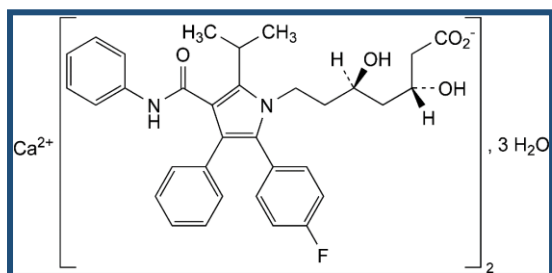


**Figure 1. Chemical structure of atorvastatin calcium** <sup>(8)</sup>.

Solid dispersion (SD) is the most generally used technique for bioavailability enhancement of poorly water-soluble drugs, as the drug is dispersed in a freely soluble carrier <sup>(9)</sup>.

Due to their amphiphilic nature, phospholipids can be technically used in oral dosage forms as emulsifiers, wetting agents, solubilizers, and liposome former. In addition, unsaturated phospholipids can be used as a carrier for solid dispersions when solubilization and fast release of the API are required, whereas saturated phospholipids may be suitable for slow-release tablet formulations <sup>(10)</sup>. The aqueous solubility of celecoxib and that of aprepitant was found to be enhanced using phospholipids (especially phosphatidylcholine) as a carrier for the preparation of solid dispersion <sup>(11,12)</sup>.

Phospholipids may exhibit high levels of adhesiveness and poor flow properties in their formulation as solid dosage forms, making them more challenging to work when compared to polymer-based solid dispersion systems. As a result, transforming phospholipid-based dispersion systems into a solid state by adding adsorbent is necessary to enhance their ease of handling and processability <sup>(13)</sup>.

In the present work, phospholipid-based solid dispersions (PSD) of ATR were prepared using phosphatidylcholine as a carrier as a trial to improve its solubility and dissolution rates in the solid state.

This carrier was selected as it has a lipid-lowering effect so that a synergistic effect may be obtained with ATR <sup>(14)</sup>.

To impart solid-state properties to the ATR-PSD system, inorganic mesoporous excipients were employed as adsorbents.

## Materials and Method

### Materials

Atorvastatin calcium (ATR) was supplied by Pioneer pharmaceutical company, Iraq, as a gift sample. Phosphatidylcholine was purchased from Shanghai, Meryer biochemical technology, China. Magnesium aluminium silicate (MAS), silicon dioxide (SiO<sub>2</sub>) 30nm, silicon dioxide 15nm and Calcium silicate were purchased from Hangzhou, Hyperchem. China.

### Method

#### Preparation of phospholipid solid dispersion

Phospholipid solid dispersions (PSD) of ATR were prepared by solvent evaporation technique. A predetermined amount of ATR and PC were dissolved in methanol. Then adsorbent was added gradually to the solution with gentle stirring using a magnetic stirrer for 1 h, in weight equal to 50% w/w to the total weight of solid dispersion (Table 1). The resulting mixture was left for 24 hours in a 40°C oven for removal of solvent. Finally, the mass was pulverized and sieved using no. 60 mesh sieve and stored in a desiccator for further use <sup>(12)</sup>.

#### Preparation of the physical mixture (PM)

By using the same ratio of the best formula, the PC and the adsorbent were mixed together by using a mortar and pestle till we get a fine powder. Then ATR was added to the resulting powder and mixed well. The PM powder was sieved using no. 60 mesh sieve to get uniform particle size.

#### Evaluation of phospholipid-solid dispersion

##### Determination of percentage yield (PY %) of the prepared PSD

The practical percentage yield (PY%) was determined for all the prepared PSD formulations. The PY% was calculated by dividing the actual mass of the PSD formula by the theoretical mass of PSD, using the equation below <sup>(15)</sup>.

$$PY\% = \frac{\text{Practical weight (PSD)}}{\text{Theoretical weight (PSD)}} \times 100 \quad \text{eq 1}$$

##### Determination of drug content of the prepared PSD

Using a 50 ml volumetric flask, an accurately weighed amount of PSD equivalent to 10 mg of ATR was dissolved in 50 ml methanol. Then after suitable dilution the solution was assayed for drug content using UV spectrophotometric method at 246 nm. The percentage of drug content in the PSD was calculated by using the equation below <sup>(7)</sup>.

$$\text{drug content \%} = \frac{\text{Actual ATR amount in PSD}}{\text{Theoretical ATR amount in PSD}} \times 100 \quad \text{eq 2}$$

**Table 1. Composition of different ATR-PSD formulas.**

Formula code	ATR (g.)	PC (g.)	MAS (g.)	SiO2 30nm (g.)	SiO2 15nm (g.)	Ca. Silicate (g.)
F1	0.5	0.5	-	-	-	-
F2	0.5	1.5	-	-	-	-
F3	0.5	2.5	-	-	-	-
F4	0.5	0.5	1	-	-	-
F5	0.5	1.5	2	-	-	-
F6	0.5	2.5	3	-	-	-
F7	0.5	0.5	-	1	-	-
F8	0.5	1.5	-	2	-	-
F9	0.5	2.5	-	3	-	-
F10	0.5	0.5	-	-	1	-
F11	0.5	1.5	-	-	2	-
F12	0.5	2.5	-	-	3	-
F13	0.5	0.5	-	-	-	1
F14	0.5	1.5	-	-	-	2
F15	0.5	2.5	-	-	-	3

**Determination of saturation solubility**

Saturated solubility was determined by adding an excess amount of pure ATR and ATR-PSDs into 10 ml of water, and incubated in a water bath shaker at 25 °C for 48 hours. The samples were filtered using a 0.45µm filter syringe and diluted when necessary<sup>(16,17)</sup>. The dissolved ATR was analyzed using UV-spectrophotometer at 240 λ max. The procedure was done in triplicate.

**In-vitro dissolution studies**

The *in-vitro* dissolution of pure ATR and PSDs was assessed using a USP apparatus II (RC-6, China) An equivalent amount of 10 mg of ATR was dispersed in 900 ml of 0.05M phosphate buffer (pH 6.8) as a dissolution media, and the temperature was maintained at 37±0.5°C using a thermostatic water bath. The apparatus was set to rotate at a speed of 75 rpm<sup>(18)</sup>. Samples were collected at regular intervals and replaced with a fresh dissolution medium. The samples were filtered and measured using spectrophotometry at 240 nm. This evaluation was conducted on the PSD formulations that exhibited the highest solubility in triplicate.

The dissolution profile was statistically analyzed using a similarity factor (*f*<sub>2</sub>) as calculated by the following equation.

$$f_2 = 50 \cdot \log \left\{ 100 \cdot \left[ 1 + \frac{1}{n} \sum_{t=1}^n (Rt - Tt)^2 \right]^{-0.5} \right\} \quad \text{eq3}$$

At time *t*, (*Rt*) represents the dissolution value of the reference, (*Tt*) represents the dissolution value of the test, and (*n*) denotes the number of dissolution time points. Dissolution profiles are deemed similar when *f*<sub>2</sub> values exceed 50 (ranging from 50 to 100), while dissolution profiles are deemed dissimilar if the *f*<sub>2</sub> value falls below 50<sup>(19)</sup>.

**Fourier Transforms Infrared Spectroscopy (FTIR)**

The FTIR spectra of pure ATR, PC, selected adsorbent, the optimal formula, and its PM were analyzed to investigate potential interactions between the drug and the component of the formula. An infrared spectrophotometer (IRAffinity-1, Shimadzu, Japan) was employed to obtain these spectra over a scanning range of 400-4000 cm<sup>-1</sup><sup>(20)</sup>.

**Powder x-ray diffraction (PXRD)**

Powder X-ray diffraction (DX2700BH, China) was used to evaluate the crystalline state of the pure ATR, PC, selected adsorbent, the selected PSD formula, and its PM. the target metals Cu, filter Kα, 40kV, and 30mA. The scan was over a 2θ range of 5-80° at 1.5406 Å wavelength<sup>(21)</sup>.

**Differential scanning calorimetry (DSC)**

Thermal characteristics were analyzed using an automatic thermal analyzer system (Setaram, DSC-131 evo, France) of the pure ATR, MAS, the selected PSD formula, and its PM. Each sample (10 mg) was placed in none hermetically aluminum pan and heated at a rate of 10°C/ min over temperatures 30°C to 300°C. The analysis was carried out under the atmosphere flow conditions<sup>(22)</sup>.

**Statistical analysis**

The mean and standard deviation (SD) of the triplicate samples were calculated and presented as the outcomes of the experiments. The statistical analysis was performed using one-way analysis of variance (ANOVA) and the test level of significance was set at (*P* < 0.05). The statistical software used for the analysis was SPSS version 26.

**Results and Discussion****Percentage yield (PY %) and drug content of prepared PSD**

Without adding adsorbent, the prepared PSDs formulas resulted in sticky mass that was

unable to sieve. Except for Calcium silicate, a high percentage yield ranging between 88.65-97.21% was obtained by adding adsorbents (Table 2). This result indicates that this method was suitable and efficient when using MAS or SiO<sub>2</sub>. Due to the lower silicon dioxide content, in calcium silicate, it may have fewer available silanol groups on its surface compared to MAS and SiO<sub>2</sub> <sup>(14)</sup>, resulting in a reduced adsorption capacity for phospholipids due

to a limited number of interaction sites. Therefore, this adsorbent was canceled from further study <sup>(23)</sup>.

On the other hand, the findings of percentage drug content fell within the range of (98.31-101.55%) w/w for all yielded formulas (Table 2), aligning with the USP guidelines of (98-102%) <sup>(18)</sup>. These observations suggest that the preparation process resulted in minimal loss of ATR with uniform dispersion within ATR-PSD formulas.

**Table 2. The practical yield percent (PY %) and drug content of ATR-PSDs using different adsorbents.**

Formula Code	Percentage yield (PY %)	Drug content (w/w) (%) (Mean ±SD) (n=3)
F1	Sticky mass	-
F2	Sticky mass	-
F3	Sticky mass	-
F4	92.57%	100.6% ±0.9
F5	88.65%	98.55% ±0.33
F6	94.10%	99.23% ±0.09
F7	96.10%	98.36% ±0.08
F8	95.80%	98.35% ±0.01
F9	97.21%	101.55% ±0.03
F10	90.60%	99.58% ±0.14
F11	97.01%	99.1% ±0.06
F12	93.23%	100.2% ±0.17
F13	Sticky mass	-
F14	Sticky mass	-
F15	Sticky mass	-

**Saturation solubility of pure ATR and ATR-PSD**

The saturation solubility study results for pure ATR

and ATR-PSD formulas are presented in Table 3.

**Table 3. The Saturation solubility of pure ATR and ATR-PSDs formulas using different Drug: PC: adsorbent ratios in distilled water at 25°C**

Formula code	(ATR: PC) and (ATR: PC: adsorbent) ratio	Saturated solubility µg/ml, Mean ±SD (n=3)
ATR		150.8±6.19
F1	ATR: PC (1:1)	193.9±2.59
F2	ATR: PC (1:3)	942.67±22.12
F3	ATR: PC (1:5)	1246±24.25
F4	ATR: PC: MAS (1:1:2)	1805.33±27.01
F5	ATR: PC: MAS (1:3:4)	3151.33±49.36
F6	ATR: PC: MAS (1:5:6)	2496.67±23.03
F7	ATR: PC: SiO <sub>2</sub> 30nm (1:1:2)	657.67±6.5
F8	ATR: PC: SiO <sub>2</sub> 30nm (1:3:4)	1603.67±5.13
F9	ATR: PC: SiO <sub>2</sub> 30nm (1:5:6)	2455.33±14.01
F10	ATR: PC: SiO <sub>2</sub> 15nm (1:1:2)	228.6±2.86
F11	ATR: PC: SiO <sub>2</sub> 15nm (1:3:4)	500.02±13.95
F12	ATR: PC: SiO <sub>2</sub> 15nm (1:5:6)	993.30±36.29

Except for F1 and F10; the solubility of ATR was significantly improved (P-value <0.05) in all PSD formulations as compared to the solubility of the pure drug.

A significant enhancement in solubility was obtained (P<0.05) by using a higher ratio of PC in PSDs. PC being an amphiphilic surfactant,

increased the solubility of the drug by the action of wetting and dispersion <sup>(11,24)</sup>.

Furthermore, a significant enhancement in solubility (P<0.05) was obtained by using an adsorbent in the formulation. This result was in alignment with the study by Rajesh S. J *et al* who found enhancement in solubility of nifedipine when adsorbed onto porous adsorbent <sup>(25)</sup>. This can be

attributed to the adsorption of the dispersion system, consisting of the drug and phosphatidylcholine, onto the high surface area and hydrophilic adsorbent material. This adsorption results in an increased surface area of the drug that is exposed to the solvent, improved wettability of the drug particles, prevention of agglomeration, and an increase in the solubility of the drug<sup>(26)</sup>. For all ATR: PC: adsorbent ratio, the order of the impact of adsorbents on improving solubility was observed to be MAS > SiO<sub>2</sub> 30nm > SiO<sub>2</sub> 15nm. This is because MAS has a multilayer of silicate resulted in a large surface area<sup>(27)</sup>.

The higher solubility of SiO<sub>2</sub> 30nm compared to SiO<sub>2</sub> 15nm can be attributed to a greater loading of ATR: PC dispersion system on silica, as it has been demonstrated that increasing pore size leads to increased drug loading<sup>(23)</sup>.

#### *In-vitro* dissolution studies

Comparative *in-vitro* dissolution of the pure ATR, F5, F9, and F12 was studied (Figure 2). These formulas were selected on the base of the solubility of the best ART: PC: adsorbent ratio for each adsorbent type. The results indicated that F5, F9, and F12 exhibited improved dissolution rates, with respective *f*<sub>2</sub> values of 27.62, 38.59, and 40.04, in comparison to pure ATR.

F5 which is composed of ATR: PC: MAS in a 1:3:4 ratio showed the highest release profile (91.65%) after 15 minutes as compared with F9 (79%), F12 (76.5%), and pure ATR (61%).

This enhancement of the dissolution profile can be explained by multiple factors, including the solubilizing effect of PC, improved wettability and dispersibility of the drug, adsorption onto MAS which has hydrophilic properties, in addition to its disintegration effect in aqueous media<sup>(13,28,29)</sup>.

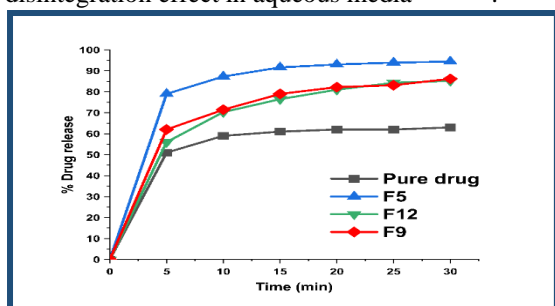


**Figure 2.** Comparison between *in-vitro* dissolution profile of the ATR, F5, F9, and F12 in 0.05M phosphate buffer (pH 6.8) at 37°C±0.5.

To prove the effectiveness of such type of solid dispersion, a comparison between F5 and its

PM was conducted. A significant improvement in dissolution rate (*f*<sub>2</sub>=37.66) demonstrates the effectiveness of the technique as shown in Figure (3)<sup>(30)</sup>.

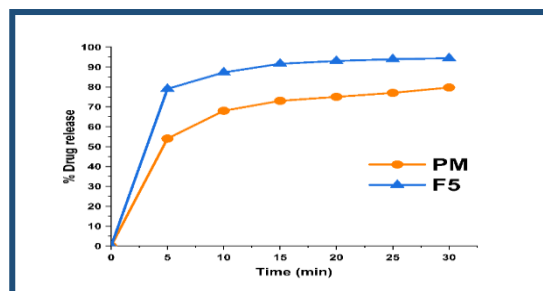


**Figure 3.** Comparison between the *in-vitro* dissolution profile of the F5 and its PM in 0.05M phosphate buffer (pH 6.8) at 37°C±0.5.

#### *Selection of the best PSD*

The (F5) formula, which combines ATR, PC, and MAS in a 1:3:4 ratio, was chosen as the best formula. It had the highest solubility and released the greatest amount of ATR in 15 minutes. This formula was subjected to further *in-vitro* evaluation studies.

#### *Evaluation of best PSD*

##### *X-ray powder diffraction (XRD)*

The XRD diffractogram of ATR, PC, MAS, F5, and its PM are shown in Figure 4. Distinctive peaks with high intensity were observed in the diffraction pattern (Braggs peaks) of the pure drug at 2 $\theta$  of 9.06°, 10.27°, 11.7°, 16.79°, 19.22°, 21.39°, 22.4°, and 23.18°, which suggests that the drug is in a crystalline state. These results were in agreement with the previous studies<sup>(26)</sup>. A notable reduction or absence of the characteristic ATR peaks was evident by comparing the XRD diffractogram of F5 with that of pure ATR and PM, suggesting the predominant presence of an amorphous state within the phospholipid solid dispersion<sup>(31)</sup>. Since the amorphous form is easier to dissolve than the crystalline form, this may explain the solubility enhancement of F5<sup>(32)</sup>.

##### *Differential scanning calorimetry (DSC)*

Thermograms of ATR, MAS, F5, and its PM are shown in Figure 5. The DSC plot for ATR demonstrates an endothermic peak observed at 168.36°C, which corresponds to its melting point<sup>(33)</sup>. This indicates the crystallinity and purity of the ATR. While the DSC thermogram of magnesium silicate exhibited a wide and gradual dehydration peak ranging between 100.6 to 140.1°C<sup>(34)</sup>, whereas no thermogram was obtained for PC as it is soft and tacky material to be operated by DSC.

While for PM, the intensity and melting point of the ATR peak decreased to 164.6°C which can be attributed to dilution with other components. This result was in agreement with that obtained by Samer A. *et al*<sup>(26)</sup>. The thermogram of F5 shows the disappearance of the ATR peak which may be due to its complete dispersion in the PC and conversion of the drug from crystalline to an amorphous state<sup>(11)</sup>.

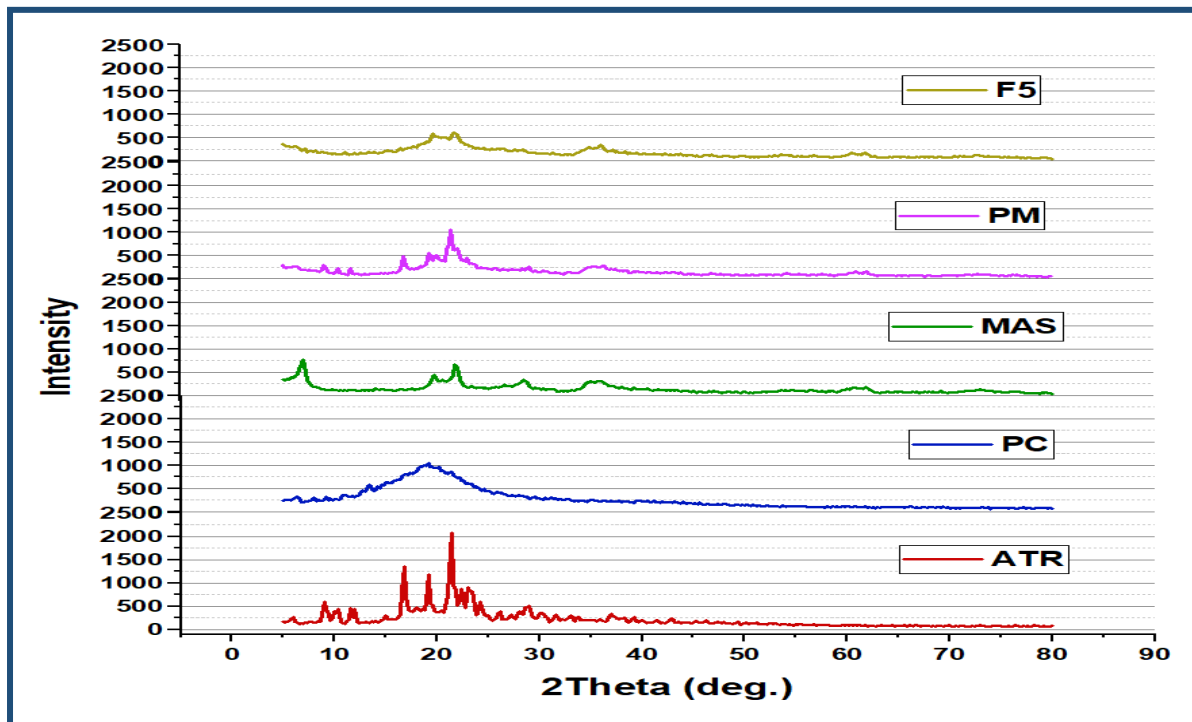


Figure 4. X-ray powder diffraction of pure ATR (Atorvastatin), PC (Phosphatidylcholine), MAS (Magnesium aluminum silicate), F5, and its PM (physical mixture).

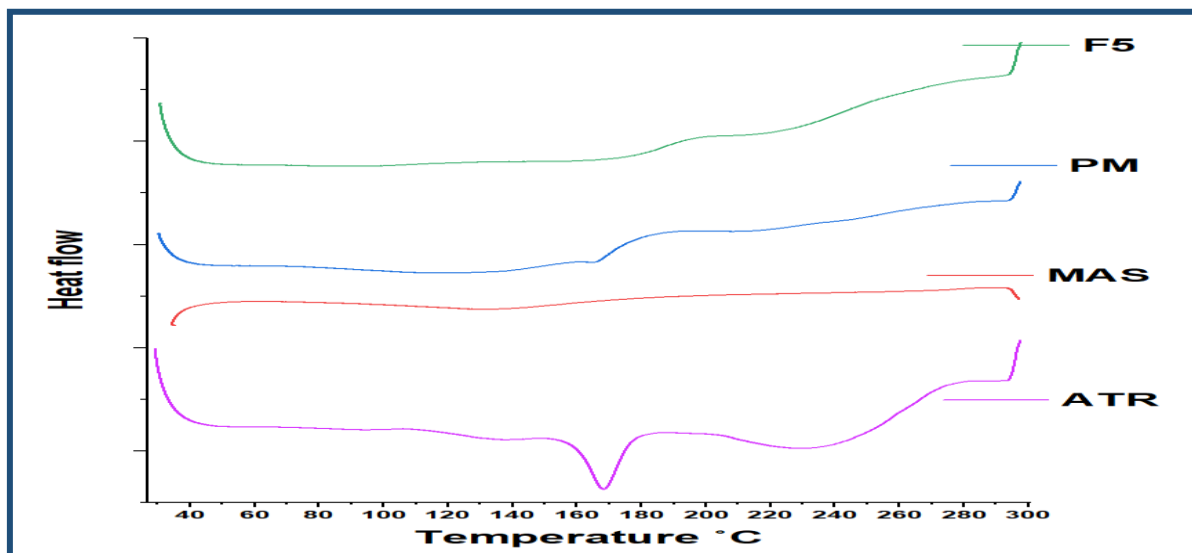


Figure 5. DSC of pure ATR(Atorvastatin), MAS (Magnesium aluminum silicate), F5, and its PM (physical mixture).

#### Fourier transform infrared

The ATR spectrum shows peaks at  $3363\text{cm}^{-1}$  (O–H stretching),  $3236\text{cm}^{-1}$  (N–H stretching),  $3055\text{cm}^{-1}$  (aromatic C–H stretching),  $2970$  and  $2920\text{cm}^{-1}$  (aliphatic C–H stretching),  $1651\text{cm}^{-1}$  (amide C=O stretching),  $1577$  and  $1550\text{cm}^{-1}$  (aromatic C=C stretching),  $1508\text{cm}^{-1}$  (N–H bending),  $744\text{cm}^{-1}$  (out of plane N–H wagging) <sup>(35)</sup> as shown in Figure 6.

While the MAS spectrum shows peaks at  $3614\text{cm}^{-1}$  (free O–H stretching),  $1635\text{cm}^{-1}$  (Si=O stretching), and  $987\text{cm}^{-1}$  (Si–O stretching) <sup>(36)</sup>.

The FTIR spectrum of PC shows peaks at  $1743\text{cm}^{-1}$  (C=O stretching),  $1450$  and  $1419\text{cm}^{-1}$  ( $\text{CH}_2$  scissoring), and  $1022\text{cm}^{-1}$  (C–O–P stretching) <sup>(37)</sup>.



Moreover, all ATR characteristic peaks are present in the PM FTIR spectrum with lower

intensity. This contributed to the dilution and predominant peaks of other components.

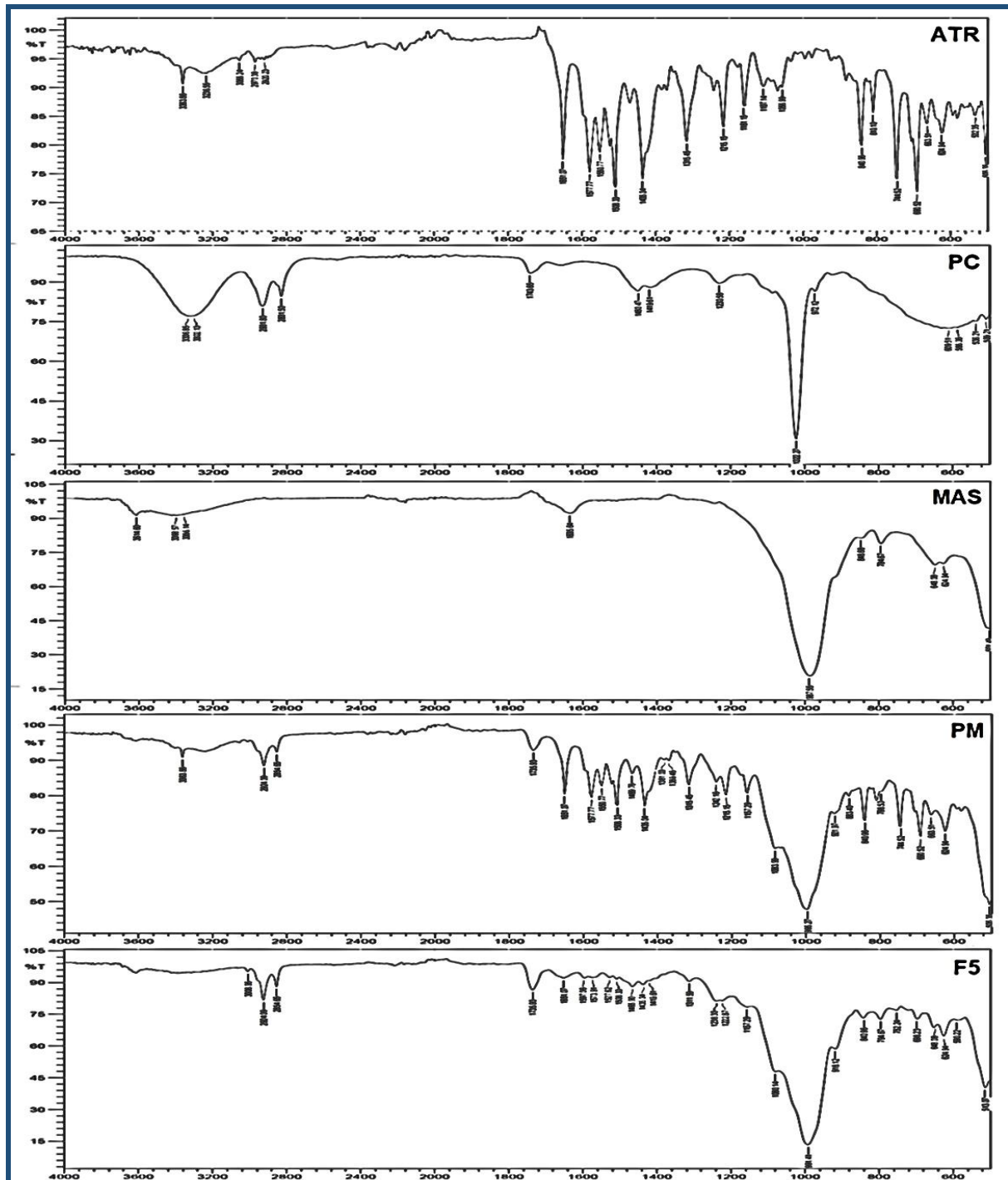


**Figure 6. FTIR Spectrum of pure ATR (Atorvastatin), PC (Phosphatidylcholine), MAS (Magnesium aluminum silicate), F5, and its PM (physical mixture).**

The stretching of the C=O bond in PC, at  $1743\text{ cm}^{-1}$ , showed a shift towards a lower wavenumber of  $1735\text{ cm}^{-1}$  in F5. Additionally, this peak exhibited reduced intensity, suggesting an electrostatic interaction between the carboxyl group of PC and positively charged sites located at the

edges of the MAS structure. Which confirms the adsorption process<sup>(38)</sup>.

The characteristic peaks of the ATR spectrum can still be observed but with a reduction in intensity, in the FTIR spectrum of F5. This suggests that there is no chemical incompatibility between the drug, PC, and MAS.

## Conclusion

PSD formulations for enhancing the aqueous solubility and dissolution rate of ATR were developed using the solvent evaporation technique with acceptable production yield. While dispersing ATR in PC alone demonstrated a significant improvement in ATR's aqueous solubility, The waxy texture of PC made it unsuitable for developing solid dosage forms. Therefore, adding adsorbent was necessary for handling the product. MAS was the best adsorbent and gave additional enhancement of aqueous solubility. In conclusion, the PSD technique demonstrate its effectiveness and efficiency technique for enhancing the solubility and dissolution rate of hydrophobic drugs.

## Acknowledgement

The authors sincerely thank the College of Pharmacy, University of Baghdad, for their valuable support in providing education and facilities that facilitated this work. An acknowledgement to Pioneer Pharmaceutical Industry for generously gifting the atorvastatin calcium and other materials used in this research.

## Conflicts of Interest

The authors declare that they have no conflicts of interest related to this work.

## Funding

The authors declare that this research received no financial support from any institution.

## Ethics Statements

According to the research integrity rules in our country, the study does not require ethical approval from an ethics committee as it's an *in-vitro* study.

## Author Contribution

All authors have actively participated in the research process and have reviewed the results. Additionally, they have approved the final version of the manuscript before submission.

## References

1. Boyd BJ, Bergström CAS, Vinarov Z, Kuentz M, Brouwers J, Augustijns P, et al. Successful oral delivery of poorly water-soluble drugs both depends on the intraluminal behavior of drugs and of appropriate advanced drug delivery systems. *European Journal of Pharmaceutical Sciences*. 2019; 137:104967.
2. Kumar S, Bhargava D, Thakkar A, Arora S. Drug carrier systems for solubility enhancement of BCS class II drugs: A critical review. *Critical Reviews in Therapeutic Drug Carrier Systems*. 2013;30(3):217–56.
3. Azemawah V, Movahed MR, Centuori P, Penafior R, Riel PL, Situ S, et al. State of the art comprehensive review of individual statins, their differences, pharmacology, and clinical implications. *Cardiovasc Drugs Ther*. 2019;33(5):625–39.
4. Moffat A, Osselton M, Widdop B. Clarke, s analysis of drug and poisons. 4th ed. London: The Pharmaceutical Press; 2011: p 930.
5. Rodde MS, Divase GT, Devkar TB, Tekade AR. Solubility and bioavailability enhancement of poorly aqueous soluble atorvastatin: *In vitro*, *ex vivo*, and *in vivo* studies. *BioMed Research International*. 2014;2014.
6. Ali AH, Abd-Alhammid SN. Enhancement of solubility and improvement of dissolution rate of atorvastatin calcium prepared as nanosuspension. *Iraqi Journal of Pharmaceutical Sciences*. 2019;28(2):46–57.
7. Hadi BM, Al-Khedairy EBH. Preparation and Characterization of Atorvastatin Calcium Trihydrate -cyclodextrin Inclusion Complex. *International Journal of Drug Delivery Technology*. 2022;12(3):1171–9.
8. British Pharmacopoeia Commission. *British Pharmacopoeia 2016: volume III*. London: TSO; 2016.
9. Khaleel NY, Abdulrasool AA, Ghareeb MM, Hussain SA. Solubility and dissolution improvement of ketoprofen by solid dispersion in polymer and surfactant using solvent evaporation method. *International Journal of Pharmacy and Pharmaceutical Sciences*. 2011;3(4):431–5.
10. Van Hoogevest P. Review – An update on the use of oral phospholipid excipients. *European Journal of Pharmaceutical Sciences*. 2017; 108:1–12.
11. Jo K, Cho JM, Lee H, Kim EK, Kim HC, Kim H, et al. Enhancement of aqueous solubility and dissolution of celecoxib through phosphatidylcholine-based dispersion systems solidified with adsorbent carriers. *Pharmaceutics*. 2019;11(1):1–14.
12. Yeo S, An J, Park C, Kim D, Lee J. Design and characterization of phosphatidylcholine-based solid dispersions of aprepitant for enhanced solubility and dissolution. *Pharmaceutics*. 2020;12(5).
13. Zhang Z, Chen Y, Deng J, Jia X, Zhou J, Lv H. Solid dispersion of berberine-phospholipid complex/TPGS 1000/SiO<sub>2</sub>: Preparation, characterization and *in vivo* studies. *International Journal of Pharmaceutics*. 2014;465(1–2):306–16.
14. Rowe R C, Sheskey P J and Quinn M E. *Handbook of pharmaceutical excipients*. eighth edition, London, Chicago, 2017. p 156-157.
15. Abdul-Rahman MM, Jawad FJ. Enhancement of aqueous solubility and dissolution rate of etoricoxib by solid dispersion technique. *Iraqi Journal of Pharmaceutical Sciences*. 2020;29(1):76–87.
16. Hussain HAM, Al-Khedairy EBH. Preparation and *in vitro* evaluation of cyclodextrin based effervescent and dispersible granules of



- carbamazepine. International Journal of Applied Pharmaceutics. 2018;10(6):290–7.
17. Tripathi D, Sharma K, Sahoo J, Chaudhary N. Tripathi D et al. A recent advancement in approaches used for estimation of drug solubility: A review. Der Pharmacia Lettre. 2020;12(4):15–29.
  18. The United State Pharmacopeia (USP) 41, NF36. Convention Inc. Rockville, MD. 2018.
  19. Muselík J, Komersová A, Kubová K, Matzick K, Skalická B. A critical overview of FDA and EMA statistical methods to compare *in vitro* drug dissolution profiles of pharmaceutical products. Pharmaceutics. 2021;13(10).
  20. Ismail MY, M. Ghareeb M. Enhancement of the solubility and dissolution rate of rebamipide by using solid dispersion technique (Part I). Iraqi Journal of Pharmaceutical Sciences. 2018;27(2):55–65.
  21. Jacobsen AC, Ejskjær L, Brandl M, Holm R, Bauer-Brandl A. Do phospholipids boost or attenuate drug absorption? *In vitro* and *in vivo* evaluation of mono- and diacyl phospholipid-based solid dispersions of celecoxib. Journal of Pharmaceutical Sciences. 2021;110(1):198–207.
  22. Abduljabbar HH, Abd Alhammid SN. Enhancement of the solubility and the dissolution rate of tamoxifen citrate solid dispersion using Soluplus by solvent evaporation technique. Asian J Pharm Clin Res. 2019;12(1):216.
  23. Choudhari Y, Hoefler H, Libanati C, Monsuur F, McCarthy W. Mesoporous silica drug delivery systems. 2014;665–93.
  24. Telange DR, Sohail NK, Hemke AT, Kharkar PS, Pethe AM. Phospholipid complex-loaded self-assembled phytosomal soft nanoparticles: evidence of enhanced solubility, dissolution rate, *ex vivo* permeability, oral bioavailability, and antioxidant potential of mangiferin. Drug Delivery and Translational Research. 2021;11(3):1056–83.
  25. Jagtap RS, Doijad RC, Mohite SK. Adsorption of nifedipine on porous calcium silicate for enhancement of solubility and dissolution rate. Research Journal of Pharmacy and Technology. 2019;12(3):1273–9.
  26. Ali SK, Al-Khedairy EBH. Solubility and dissolution enhancement of atorvastatin calcium using solid dispersion adsorbate technique. Iraqi Journal of Pharmaceutical Sciences. 2019;28(2):105–14.
  27. Totea AM, Dorin I, Laity PR, Sabin J, Conway BR, Waters L, et al. A molecular understanding of magnesium aluminum silicate – drug, drug–polymer, magnesium aluminum silicate – polymer nanocomposite complex interactions in modulating drug release: Towards zero order release. European Journal of Pharmaceutics and Biopharmaceutics. 2020; 154:270–82.
  28. Yoshie K, Yada S, Ando S, Ishihara K. Chemical structural effects of amphiphatic and water-soluble phospholipid polymers on formulation of solid dispersions. Journal of Pharmaceutical Sciences. 2021;110(8):2966–73.
  29. Ahmed A, Ali SA, Hassan F, Ayub S, Haque N. Effect of disintegrants and hardness on the disintegration time of Acetaminophen tablets. Pakistan journal of pharmaceutical sciences. 1998;11(1):41–6.
  30. Chen X, Partheniadis I, Nikolakakis I, Al-Obaidi H. Solubility improvement of progesterone from solid dispersions prepared by solvent evaporation and co-milling. Polymers (Basel). 2020;12(4).
  31. Fong SYK, Martins SM, Brandl M, Bauer-Brandl A. Solid phospholipid dispersions for oral delivery of poorly soluble drugs: Investigation into celecoxib incorporation and solubility *in-vitro* permeability enhancement. Journal of Pharmaceutical Sciences. 2016;105(3):1113–23.
  32. Alshehri S, Imam SS, Hussain A, Altamimi MA, Alruwaili NK, Alotaibi F, et al. Potential of solid dispersions to enhance solubility, bioavailability, and therapeutic efficacy of poorly water-soluble drugs: newer formulation techniques, current marketed scenario and patents. Drug Delivery. 2020;27(1):1625–43.
  33. Sonje VM, Kumar L, Meena CL, Kohli G, Puri V, Jain R, et al. Atorvastatin calcium. Al-Majed AA. Profiles of Drug Substances, Excipients and Related Methodology. Elsevier Inc.; 2010. 1–70 p.
  34. Al-Akayleh F, Al-Mishlab M, Shubair M, Alkhatib HS, Rashid I, Badwan A. Development and evaluation of a novel, multifunctional, coprocessed excipient via roller compaction of  $\alpha$ -lactose monohydrate and magnesium silicate. Journal of Excipients and Food Chemicals. 2013;4(2):27–37.
  35. Alrasheed A.W. Mohammed, Salah Elnaiem Mohammed HSB, Abdelmula MH, Hammad MHAMOM and AMA. Development and validation method for the determination of atorvastatin Development and validation method for the determination of atorvastatin calcium tablets drugs by using UV spectrophotometer in pharmaceutical calcium tablets drugs by using UV-spectro. Research Journal of Pharmaceutical Sciences. 2019;8(1):5–14.
  36. Treto-Suárez MA, Prieto-García JO, Mollineda-Trujillo Á, Lamazares E, Hidalgo-Rosa Y, Mena-Ulecia K. Kinetic study of removal heavy metal from aqueous solution

- using the synthetic aluminum silicate. *Scientific Reports*. 2020;10(1):1–13.
37. Hindarto CK, Surini S, Permana AH, S SR, Irawan C. Effect of mole ratio on physicochemical properties of luteolin-loaded phytosome. *The Pharma Innovation Journal*. 2017; 6:96–101.
38. Pongjanyakul T, Pripem A, Puttipatkhachorn S. Investigation of novel alginate-magnesium aluminum silicate microcomposite films for modified-release tablets. *Journal of Controlled Release*. 2005;107(2):343–56.



This work is licensed under a [Creative Commons Attribution 4.0 International License](https://creativecommons.org/licenses/by/4.0/).